A NOVEL SIMPLE ADAPTIVE SPECTRAL ANALYSIS ZOOM FOR NARROW–BAND SIGNALS

Abdulnasir Hossen

Information Engineering Department
Sultan Qaboos University
P.O.Box 33 Al-khod
Muscat,123 Oman
abhossen@squ.edu.om

Ulrich Heute

Institute for Circuits and Systems Theory
Christian–Albrechts University
Kaiserstrasse 2
24143 Kiel, Germany
uh@techfak.uni-kiel.de

ABSTRACT

In [1] a new spectral analysis zoom technique for narrow–band signal applicationns was presented. This zoom–technique is based on subband decomposition and linear prediction. The subband–decomposition idea applied to both FFT [2], [3] and DCT [4], [5] to find these transforms with less computations, is used in [1] in combination with the linear prediction algorithm to implement a new zoom technique with higher spectral resolution efficiency than other techniques. In this work the new algorithm computational complexity is studied. The zoom capability of this subband decomposition zoom technique is also explained by considering many factors such as the gain of the linear prediction modelling and the power spectral density and autocorrelation between the linear prediction coefficients [6]. The accuracy of the technique in terms of the prediction error and minimum allowable signal to noise ratio is also included in this paper. Finally, the adaptive capabilty of the subband–FFT is included in the zoom algorithm to select the band of most energy (the band to be zoomed).

1. INTRODUCTION

The subband FFT (SB–FFT) is a fast and approximate method, in which the transform can be obtained by decomposing the input sequence into two bands corresponding to low– and high–pass sequences. One of the two bands (the band with the larger energy) is to be transformed while the other one is to be ignored. The SB–FFT computes the frequency spectrum in a small band but with the same resolution obtained using the full–band FFT [7]. Parametric methods of spectral analysis are three step procedures. The first step is to select a model. The second step is to estimate the parameters of the assumed model using the available data samples. The third step is to obtain the spectral estimate by substituting the estimated model parameters into the theoretical PSD implied by the model [8], [9].

In [1] the combination of the two advantages, the smaller complexity of the SB–FFT and the high resolution of the linear prediction algorithm, yields a new spectral analysis zoom technique for narrow–band signal applications. In this paper the complexity and the zoom capability of the new zoom technique are investigated. A simple adaptive search algorithm to determine the band of interest out of many bands is included in the zoom.
The paper is organized as follows:
In the next section the linear prediction parametric method of spectral analysis is reviewed. Section 3 introduces the adaptive SB–FFT method [10]. In section 4, the new zoom technique is investigated. Results of complexity analysis and zoom capability of the algorithm is also given in this section. The modification of the algorithm to find adaptively the band to be zoomed is included in section 5. Conclusions of the results are given in section 6.

2. LINEAR PREDICTION

A linear prediction coding process generates an all–pole recursive filter, whose impulse response matches a given sequence. It assumes that each output sample of a signal $x(n)$ is a linear combination of the past p samples (that is, it can be lineary predicted from these outputs) [6]:

$$x(n) = -c(1)x(n-1) - c(2)x(n-2) - \cdots - c(p)x(n-p). \quad (1)$$

The coefficients of the last equation are found, e.g., by the autocorrelation method of all–pole modelling of order p. This technique is also called the Yule-Walker AR method of spectral analysis [6]. The filter coefficients might not model the signal exactly, because the autocorrelation method implicitly windows the data (it assumes samples beyond the length of the sequence x are 0) [9]. After the coefficients of the recursive digital filter are found, the frequency response of the filter

(equivalent to the frequency spectrum of the time series x) can also be found by classical spectrum–analysis methods [11].

3. SUBBAND–FFT

The signal $x(n)$ is decomposed in Fig.1 into two subsequences corresponding to the low–pass $a(n)$ and the high–pass $b(n)$ sequences in the upper–branch and lower–branch of the figure, respectively. After down–sampling by 2, $g(n)$ and $h(n)$ are obtained:

$$\begin{aligned} g(n) &= \frac{1}{2}[x(2n) + x(2n+1)] \\ h(n) &= \frac{1}{2}[x(2n) - x(2n+1)]. \end{aligned} \quad (2)$$

The exact full–band size–N DFT $X(k)$ can be obtained by [2], [3]:

$$X(k) = (1 + W_N^k)F_g(k) + (1 - W_N^k)F_h(k). \quad (3)$$

If only the low–pass band sequence is to be followed (depending on a–priori information about the energy distribution of the signal), $X(k)$ can be approximated as:

$$X(k) \approx (1 + W_N^k)F_g(k), \qquad k \in (0, 1, ..., N/4 - 1). \quad (4)$$

The decomposition process in Fig.1 can be applied m times to obtain $M = 2^m$ subbands, out of which only one band is to be computed depending on the information (known a priori or derived from the signal) about the input signal power distribution [10].

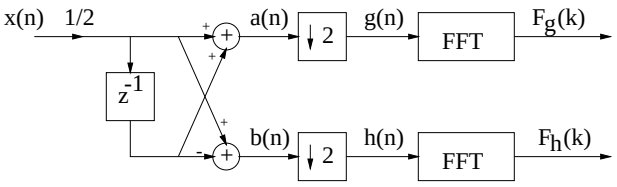

Figure 1: Two–band decomposition of the subband DFT

If there is no a-priori information about the concentration of the signal energy in the different frequency bands, a simple adaptive algorithm can be inserted into the SB–DFT computations [10]. A comparison between the energy of the low– and high–frequency subsequences $g(n)$ and $h(n)$ given by Eq.(2) is performed by finding:

$$sgn(B) = sgn \sum_{n=0}^{N/2-1} |g(n)| - |h(n)|. \quad (5)$$

According to $sgn(B)$, the decision will be taken: If B is positive, the low–frequency band will be calculated, and if B is negative, the high–frequency band will be calculated.

4. NEW ZOOM TECHNIQUE

4.1. Basic Idea

The newly introduced zoom technique is obtained by performing the following steps [1]:

1. Subband decomposition of the input signal applying the simple filters in Fig.1. The decomposition can be repeated till finding the band of interest.
2. Calculating the c coefficients of the IIR filter (p–th order) in Eq.(1) from the subsequence obtained from the previous step.
3. Calculating the frequency spectrum using the resulting c coefficients.

In Fig.2, the spectrum of two adjacent frequencies 10 Hz and 15 Hz is found with a sampling frequency of 2000 Hz. A linear prediction of order $p = 10$ is implemented for different values of M. $M = 1$ is corresponding to the direct linear prediction for a signal length of $N = 2048$, while the other cases are representing a linear prediction for a single–band out of M bands with a signal length of N/M.

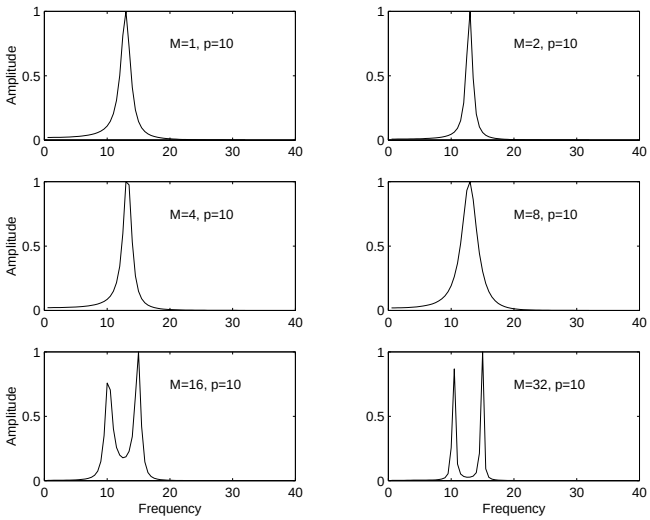

Figure 2: New zoom spectral analysis results for different M

4.2. Investigation

The linear–prediction coefficients c of the above cases, plotted in Fig.3, show more information at higher M. Table 1 shows different values related to the coefficients c for 6 different values of M. The gain factor GF is proportional to the amount of error in the prediction process of the input signal. When the number M of subbands increases, the gain also increases showing

more prediction error since the number of points used in the prediction decreases. But still it is clear from Fig.2 that a better spectrum resolution is obtained as M increases because at each stage of the decomposition the down–sampling process reduces the sampling frequency and thus increases the sampling period and causes better frequency resolution [8]. Values of $SPSD$ (sum of power spectral density of the linear prediction coefficients c) and SAC (sum of autocorrelation of the c coefficients) are increasing with M indicating better frequency performances.

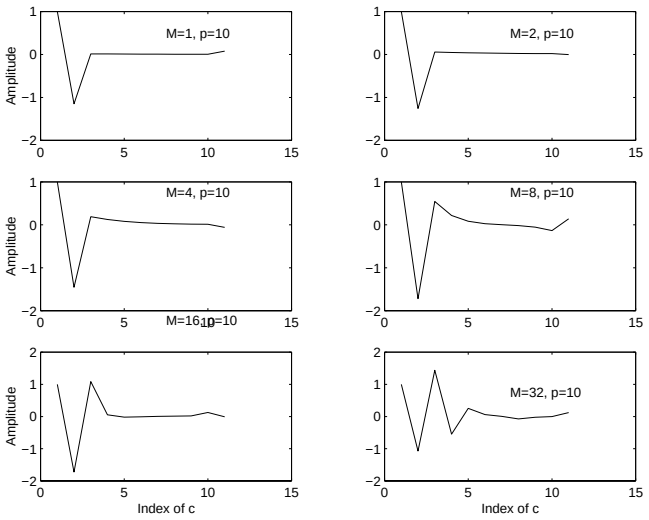

Figure 3: Linear prediction coefficients of Fig.2

$Method$	GF	$SPSD$	SAC
$M = 1$	0.64	0.1586	0.000158
$M = 2$	0.645	0.3213	0.00039
$M = 4$	0.8378	0.6907	0.0039
$M = 8$	1.225	1.663	0.1098
$M = 16$	1.844	3.578	0.749
$M = 32$	2.305	0.5276	3.253

Table 1: Different factors for the linear prediction coefficients

4.3. Modelling Accuracy

To compare the modelling accuracy of the linear prediction with different values of M with that obtained with $M = 1$, the original signal is reconstructed from the linear prediction coefficients c. This can be performed by computing the impulse response of the digital filter with numerator coefficients 1 and denominator coefficients c, N/M points are calculated in each case. The prediction error is the difference between the original signal values and the computed filter impulse response values. In Table 2, the values of the square of the prediction error normalized with the length of the signal are listed for different values of M and p.

$Method$	$p = 5$	$p = 10$	$p = 20$	$p = 50$	$p = 100$
$M = 1$	3.26	3.345	3.28	3.017	2.21
$M = 2$	3.45	3.426	3.34	2.338	1.26
$M = 4$	2.248	2.206	1.828	0.698	0.33
$M = 8$	1.428	1.196	0.609	0.2484	0.175
$M = 16$	0.8845	0.541	0.363	0.2742	0.25
$M = 32$	0.6310	0.3232	0.283	0.2403	0.19

Table 2: The normalized square of the prediction errors for differents M and p

4.4. Computational Complexity

In Table 3, the execution times of the new zoom technique are listed for different values of N and M. All values are normalized with respect to the execution time of the new zoom technique with $N = 4096$ and $M = 1$.

$Method$	$N = 4096$	$N = 2048$	$N = 1024$	$N = 512$
$M = 1$	1	0.47	0.221	0.103
$M = 2$	0.275	0.129	0.060	0.028
$M = 4$	0.132	0.062	0.029	0.0136
$M = 8$	0.065	0.03	0.0143	0.0068
$M = 16$	0.0335	0.0158	0.0076	0.0036
$M = 32$	0.0188	0.009	0.0044	0.0022

Table 3: Zoom technique computational complexity

4.5. Zoom–Capability

Table 4 shows the zoom capability of the zoom technique for different values of M in the presence of additive white noise. The minimum allowable SNR for each case of M is measured by keeping the signal amplitudes constant and increasing the noise signal till the zoom fails to discriminate between the two adjacent frequecies 10 Hz and 15 Hz, N is taken to be 2048 and $p = 100$, $f_s = 2000$ Hz. The zoom at high values of M operates more efficiently because of its high prediction capability, although the aliasing errors (caused by the noise signal) are increasing with M.

5. ADAPTIVE ZOOM TECHNIQUE

Fig.4 shows the results of applying the adaptive selectivity of the subband–FFT in the new zoom technique to separate between two adjacent frequencies located at any frequency band using different values of M. In Fig.4a and Fig.4b, the adaptive zoom is implemented to compute the spectrum of two adjacent frequencies

$Method$	SNR in dB
$M = 1$	7
$M = 2$	-9.3
$M = 4$	-11.7
$M = 8$	-12.9
$M = 16$	-14
$M = 32$	-16

Table 4: Minimum allowable SNR for different values of M

20 Hz and 30 Hz with $M = 4$ (low–low) frequency–band and $M = 8$ (low–low–low) frequency–band respectively. In Fig.4c and Fig.4d, two frequencies of 270 Hz and 280 Hz are computed with $M = 4$ (high–low) band and $M = 8$ (high–low–low) band respectively.

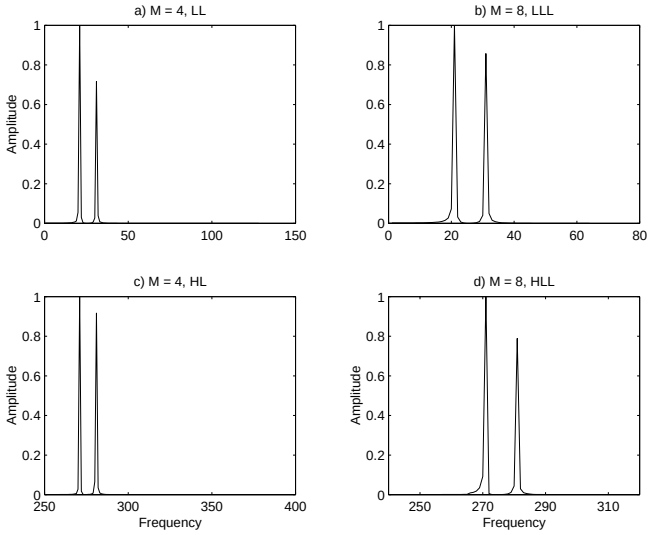

Figure 4: New adaptive zoom technique examples

6. CONCLUSIONS

A new zoom technique for spectral–analysis applications is introduced in the paper. This technique combines the advantages of subband decomposition (reduction in complexity and zoom capability) and linear prediction (better resolution). It has been shown that as the number of subbands increases, the spectral resolution improves accordingly without increasing the transform length. This is due to higher values of SPSD and SAC in Table 1 and smaller prediction errors in Table 2. The new zoom technique is shown to be very efficient in presence of noise. The minimum allowable SNR is found to be 7 dB for $M = 1$. This value is decreased to about -16 dB at $M = 32$. So at higher M better zoom capability are obtained with less computational complexity (see Table 3). Lastly, the very important addition to the zoom technique is its adaptive ability to find the band of higher energy (to be zoomed).

AKNOWLEDGMENT

This work was supported by DAAD (German Academic Exchange Service) and Sultan Qaboos University at Muscat, Sultanate of Oman.

REFERENCES

[1] Hossen, A.; and Heute, U., "A New Spectral Analysis Zoom Technique Based on Subband Decomposition and Linear Prediction ", Proceedings of ECMCS 2001, Budapest, Hungary.

[2] Shentov, O.; Mitra, S.; Heute, U.; Hossen, A., "Subband DFT–Part I: Definition, Interpretation and Extensions", Signal Processing, Vol.41, no.3, Feb. 1995, pp.261-277.

[3] Hossen, A.; Heute, U.; Shentov, O.; and Mitra, S., "Subband DFT–Part II: Accuracy, Complexity, and Applications", Signal Processing, Vol. 41, no.3, Feb. 1995, pp.279–294.

[4] Jung, S.; Mitra, S.; and Mukherjee, D., "Subband DCT: Definition, Analysis, and Applications", IEEE Trans. on Circuits and Systems for Video Technology, Vol.6, N0.3, June 1996.

[5] Hossen, A.; and Heute, U., "General Adaptive Sub–Band DCT", Proceedings of ECSAP–97, Prague, Czech Republic, June 1997.

[6] "Matlab Signal Processing Toolbox," The MathWorks 1996.

[7] Hossen, A.; and Heute, U., "Different Approaches for a High Resolution Narrow–Band Spectrum", Proceedings of the 7th European Signal Processing Conf.(EUSIPCO'94), Edinburgh, UK, 1994.

[8] Marple, S. Lawrence, "Digital Spectral Analysis with Applications", Prentice Hall, 1987.

[9] Kay, M. Steven, "Modern Spectral Estimation Theory and Applications", Prentice Hall, 1988.

[10] Hossen, A.; and Heute, U., "Fully Adaptive Evaluation of SB–DFT", Proceedings of IEEE Int. Symp. on Circuits and Systems, Chicago, Illinois, 1993.

[11] Oppenheim, A. V.; and Schafer, R. W.," Discrete–Time Signal Processing", Prentice–Hall, 1989.